



ELSEVIER

Dynamics of Atmospheres and Oceans 23 (1996) 299–308

---

---

dynamics  
of atmospheres  
and oceans

---

---

# The structure of the turbulent wake and the random internal wave field generated by a moving sphere in a stratified fluid

P. Bonneton <sup>a,\*</sup>, J.M. Chomaz <sup>b</sup>, E. Hopfinger <sup>c</sup>, M. Perrier <sup>d</sup>

<sup>a</sup> *Institut de Mécanique des Fluides de Toulouse, avenue du Professeur Camille Soula, 31400 Toulouse, France*

<sup>b</sup> *LADHYX, Ecole Polytechnique, 91128 Palaiseau-Cedex, France*

<sup>c</sup> *Laboratoire des Ecoulements Geophysiques et Industriels, IMG BP 53, 38041 Grenoble-Cedex, France*

<sup>d</sup> *METEO-FRANCE, 42 avenue Coriolis, 31057 Toulouse, France*

Received 2 July 1994; revised 18 January 1995; accepted 25 January 1995

---

## Abstract

We present experimental results on the structure of the turbulent wake of a sphere and on the frequencies associated with the vortex shedding in a stratified fluid. The strong correlation between the random internal wave field emitted by the wake and the coherent structures of the turbulent wake is demonstrated.

---

## 1. Introduction

In this paper probe measurements are presented which provide novel information about the internal wave field and the turbulent wake generated by a moving sphere in a stratified fluid. It completes previous work, which dealt with the structure of the near wake (Chomaz et al., 1993a, hereinafter referred to as CBH), the far wake (Chomaz et al., 1993b) and the internal wave field (Bonneton et al., 1993, hereinafter referred to as BCH). In this paper we focus on the temporal evolution of the turbulent wake structure and its interactions with the random internal wave field.

Experiments were conducted in two different water towing tanks of respective sizes  $0.5 \times 0.5 \times 4 \text{ m}^3$  and  $1 \times 3 \times 20 \text{ m}^3$ . These tanks were filled with a linear salt

---

\* Corresponding author.

stratification  $N \in [0.67, 2.02 \text{ rad s}^{-1}]$ ,  $N = (-g/\rho d\rho/dz)^{1/2}$ . Four spheres of radii  $R = \{1.12, 2.5, 3.6, 5.0 \text{ cm}\}$  were used in the experiments, and their velocities  $U$  ranged from 1 to 50  $\text{cm s}^{-1}$ . The Froude number ( $F = U/NR$ ) was varied between 0.8 and 12.7, and the Reynolds number ( $\text{Re} = U(2R)/\nu$ ), between 380 and 30 000. When, for a given stratification and a given sphere, the velocity is varied, the two dimensionless numbers  $F$  and  $\text{Re}$  vary together; the linear relation is  $\text{Re}(F) = \text{Re}(1)F$ , where  $\text{Re}(1) = 2R^2N/\nu$  is the Reynolds number for  $F = 1$ . In this paper, a set of experiments is characterized by its  $\text{Re}(1)$  value. The experimental methods have been presented in detail in CBH and BCH.

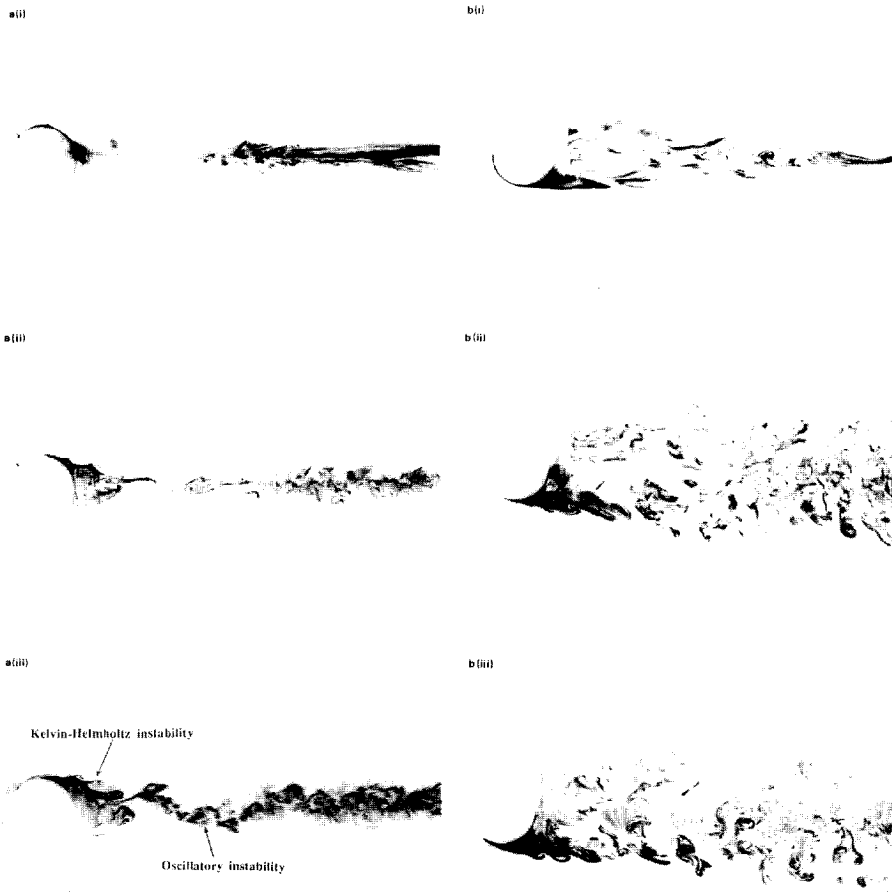


Fig. 1. Fluorescence induced by laser visualizations in (a) the vertical central plane, and (b) the horizontal central plane, for  $\text{Re}(1) = 1820$ . (i)  $F = 1$ ; (ii)  $F = 1.5$ ; (iii)  $F = 2$ .

## 2. Wake instability

CBH showed that for  $F > 4.5$  (3-D regime) the stratification has no effect on the near wake ( $Nt < 2.5$ ). As in a homogeneous fluid, a regular spiral instability occurs with a fixed Strouhal number of 0.17. Oppositely, for  $F < 1.5$  (SLW regime), the wake is dominated by a very strong lee wave of maximum amplitude  $R/2$ , which suppresses the wake instability. Between these two regimes, a more complex regime (T regime) exists, where the wake recovers progressively its behaviour in the homogeneous fluid as  $F$  increases. Horizontal and vertical laser-induced fluorescence images of the wake (Fig. 1) show that this instability does not correspond to a spiral instability but to a vertical oscillation. Lin et al. (1992b) observed a symmetric vortex shedding because they used a shadowgraph technique which is not suited to analysing precisely the structure of three-dimensional wakes. The shadowgraph picture integrates the information along each ray and the global symmetry of the picture they obtained does not imply that the wake is locally symmetric with respect to the median horizontal plane.

Conductivity probe measurements have been carried out to complete the analysis of this regime. The Strouhal number ( $S = 2fR/U$ ) of the wake instabilities is plotted in Fig. 2 as a function of  $F$ . The oscillatory vertical instability starts at  $F = 0.9$  (SLW regime), but as indicated in Fig. 3, its amplitude  $A$  is very small until  $F = 1.2$ . Moreover, for  $F \in [0.9, 1.2]$ , the instability is intermittent and very sensitive to perturbation, such as oscillations of the sphere at start up. The oscillatory instability is strongly established for  $F > 1.2$  and its Strouhal number

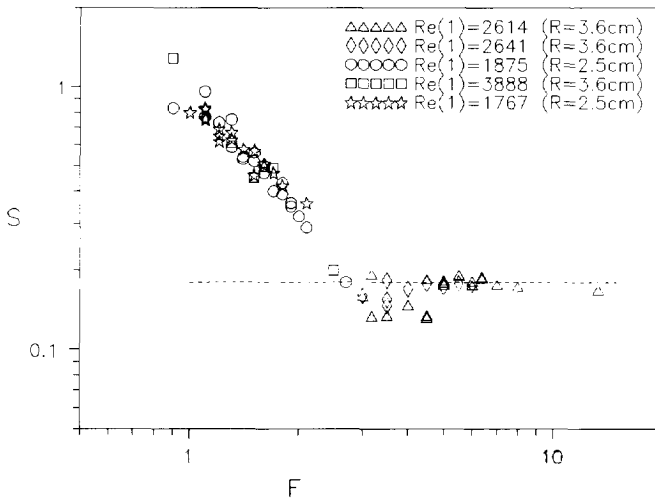


Fig. 2. Strouhal number of low-frequency instabilities of the wake as a function of the Froude number, determined from spectral analysis of velocity and conductivity probe signals. The probe is located at  $z = 0$  and  $x = 3R$ .

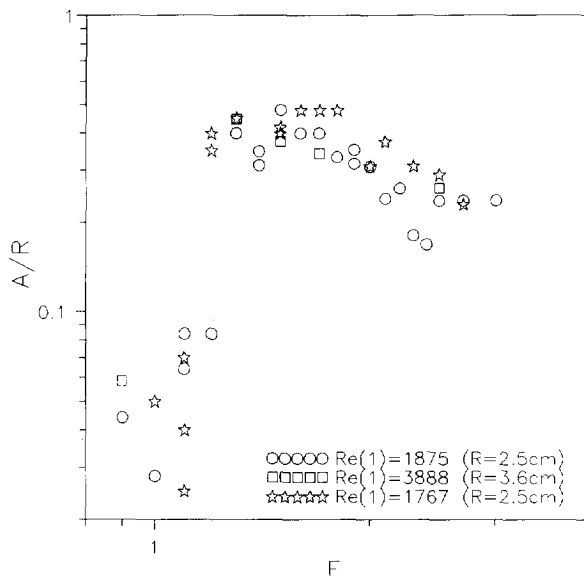


Fig. 3. Instability amplitude  $A$ , normalised by  $R$ , as a function of  $F$ , measured with a conductivity probe at the location  $z = 0$  and  $x = 3R$ .

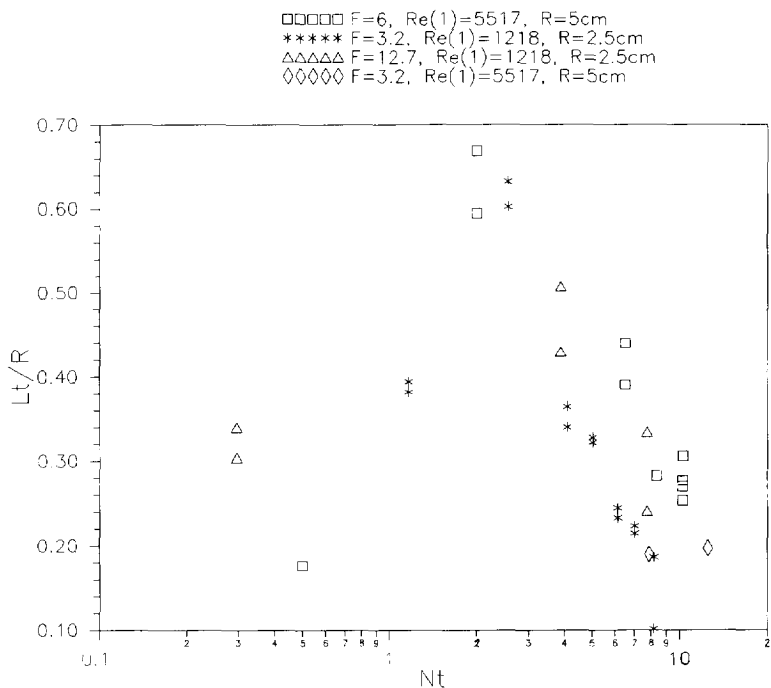


Fig. 4. Overturning length scale normalised by  $R$ , as a function of  $Nr$ .

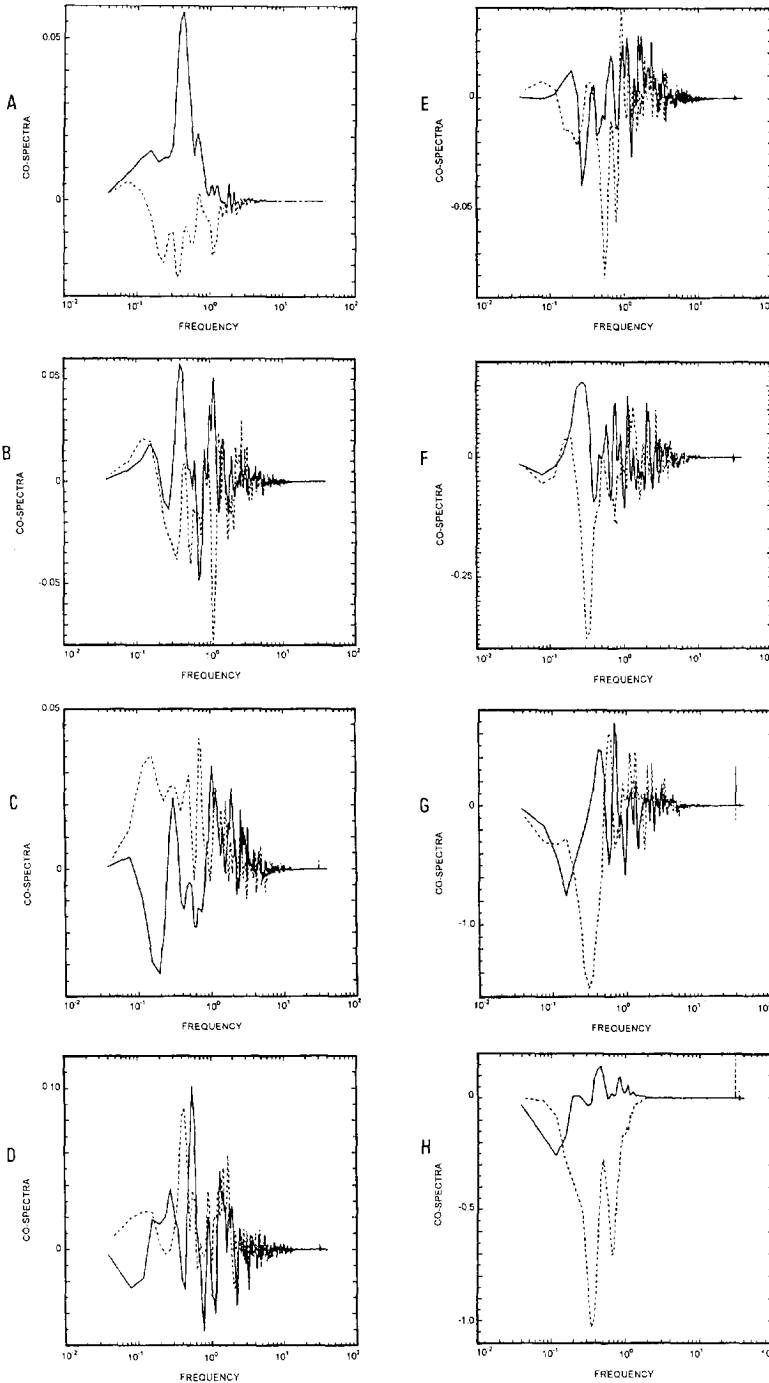


Fig. 5. Co-spectrum (solid line) and quadrature-spectrum (dashed line) of  $w'$  and  $\rho'$ , for  $F = 10/\pi$  ( $Re(1) = 1218$ ,  $R = 2.5$  cm and  $N = 1.13$  rad  $s^{-1}$ ), inside the wake at the location  $z = 0$ : (a)  $Nt = 1.2$ ; (b)  $Nt = 2.2$ ; (c)  $Nt = 4$ ; (d)  $Nt = 5$ ; (e)  $Nt = 6$ ; (f)  $Nt = 7$ ; (g)  $Nt = 8$ ; and outside the wake at the location  $z = 2R$ : (h)  $Nt = 7$ . Results are reproduced from work by Thual et al. (1987).

decreases like  $1/F^{3/2}$  until  $F \approx 3$ . The data dispersion for  $F \in [3,4.5]$  is probably related to the transition between the oscillatory instability and the spiral instability. These instabilities do not depend on the Reynolds number, except for the critical Froude number  $F_c$ , at which the instability starts ( $F_c = 0.8$  for  $\text{Re}(1) = 3888$ ,  $F_c = 0.9$  for  $\text{Re}(1) = 1875$ ,  $F_c = 1.4$  for  $\text{Re}(1) = 329$ ), and contrary to Lin et al.'s (1992b) analysis, they can not be associated with Kelvin–Helmholtz instability which leads to smaller structures also visible in Fig. 1. The transition at  $F \approx 1.2$  has been detected from measurements at location  $x = 3R$  which corresponds to  $Nt = (x/R)(1/F) \approx 2.5$ . This value coincides with the time from which the wake feels the stratification effects (see the next section and also Lin et al. (1992a)). Complementary conductivity measurements at locations  $x = 2R$  and  $4R$  have demonstrated that this transition, in fact, is independent of the probe location.

### 3. Turbulent wake structure

In this chapter we present results concerning the temporal evolution of turbulent wakes for the T and 3-D regimes. A single-electrode conductivity probe was pulled behind the sphere at several locations behind the sphere. We made also some simultaneous measurements of the vertical velocity  $w$  and of the density  $\rho$  at the same location inside and outside the wake.

The overturning length scales  $Lt = -2\langle \rho'^2 \rangle^{1/2} / (d\rho/dz)$ , where  $\rho'$  is the density fluctuation, are plotted versus  $Nt$  in Fig. 4. Similar to what is observed in homogeneous turbulence,  $Lt$  increases first with time, until  $Nt_c \approx 2.5$  and then

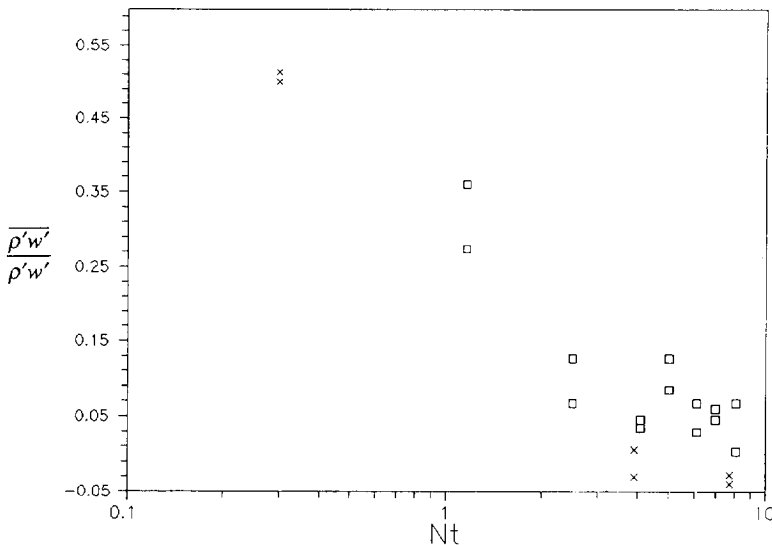


Fig. 6.  $w'$  and  $\rho'$  correlation, measured on the  $x$ -axis, as a function of  $Nt$ ;  $\square$ ,  $F = 10/\pi$ ;  $\times$ ,  $F = 40/\pi$ ;  $\text{Re}(1) = 1218$ ,  $R = 2.5$  cm and  $N = 1.13$  rad  $\text{s}^{-1}$ .

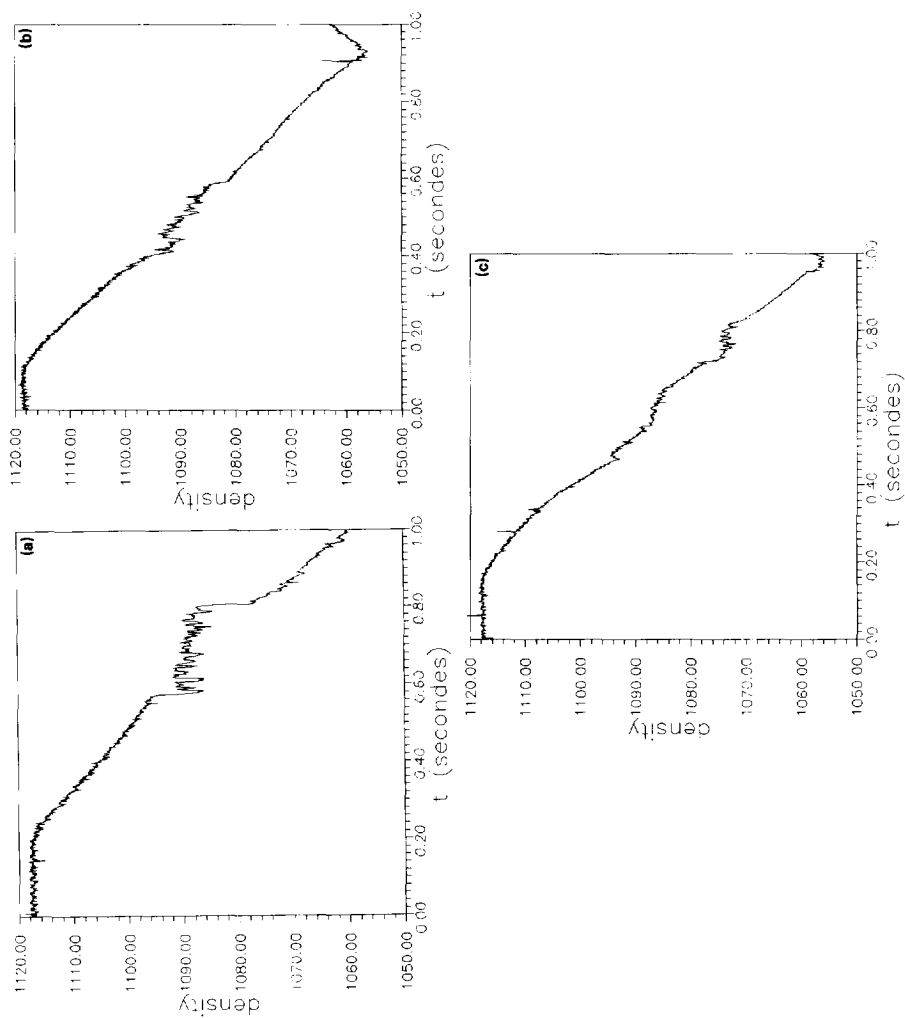


Fig. 7. Vertical density profile for  $F = 6$  ( $\text{Re}(l) = 31552$ ,  $R = 5$  cm,  $N = 1.22 \text{ rad s}^{-1}$ ); (a)  $Nt = 2$ ; (b)  $Nt = 6.5$ ; (c)  $Nt = 12$ .

starts to decrease. This transition corresponds to the maximum of the vertical wake thickness determined by Lin et al. (1992a). For  $Nt > Nt_c$ , the wake feels the stratification effects and loses its axisymmetry. The decrease of  $Lt$  with time indicates the decrease of the amplitude of vertical motions which are progressively suppressed by stratification.

Fig. 5 shows the temporal evolution of the co-spectrum and quad-spectrum of  $w'$  (the vertical velocity fluctuation) and  $\rho'$ , inside the wake ((a)–(g)) and outside the wake (h). In Fig. 5(a) the quadrature-spectrum is close to zero and the co-spectrum exhibits a significant peak which corresponds to the wake instability with a dimensionless frequency of 0.2. This implies that  $w'$  and  $\rho'$  are correlated inside the turbulent region. For  $Nt \geq Nt_c$  (Figs. 5(b)–(d)), we note that the spectrum is not dominated by the wake instability. Fig. 6 shows that  $w'$  and  $\rho'$ , measured on the  $x$ -axis, are correlated for  $Nt < Nt_c$  and uncorrelated for  $Nt > Nt_c$ .

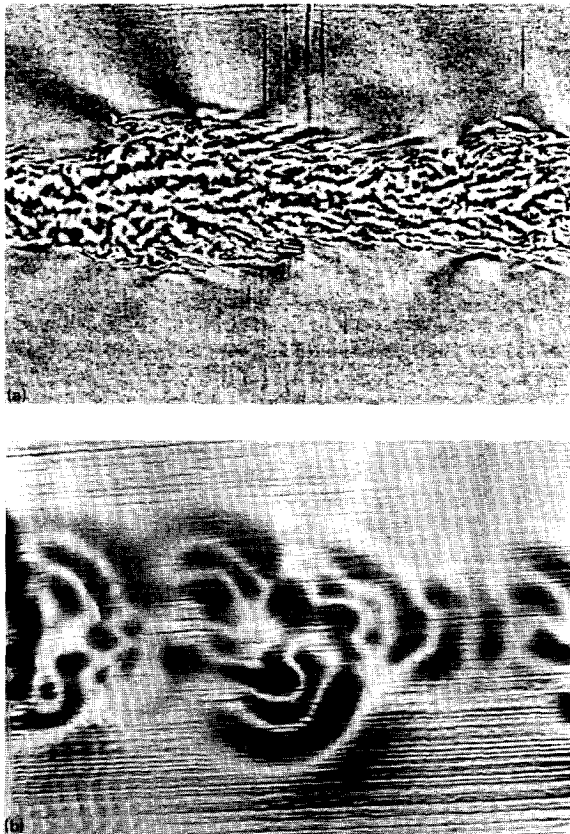


Fig. 8. Random internal wave for  $F = 20/\pi$  and  $Nt = 11$ . (a) Shadowgraph side view,  $Re = 12624$ ; (b) laser-induced-fluorescence visualization in a horizontal plane at  $z = 3R$  below the centre of the sphere,  $Re = 1611$ .



For  $Nt \geq Nt_w = 6$  (Figs. 5(e)–(g)), we observe that the quad-spectrum is large compared with the co-spectrum. This indicates that  $w'$  and  $\rho'$  oscillate in phase quadrature as required for internal waves. Thus for  $Nt \geq Nt_w$ , the wake is dominated by internal wave motions. The quadrature-spectrum shows a peak which corresponds to the wake instability frequency. This confirms the fact previously described in BCH, that the random internal wave field is generated by the collapse of the coherent structure periodically emitted by the turbulent wake. The dimensionless time  $Nt_w$  corresponds also to the time of the appearance of the internal wave outside the turbulent wake as determined by BCH.

To improve our understanding of the collapse phenomenon we measured the vertical density profile of the wake at different locations (Fig. 7). A conductivity probe was towed behind the sphere and was driven down across the wake with a constant velocity:  $43.7 \text{ cm s}^{-1}$ . In Fig. 7(a), for  $Nt$  close to  $Nt_c$ , we observe that the wake has been entirely mixed by the turbulent motions. Fig. 7(b), obtained at  $Nt > Nt_c$ , shows that the density profile is close to the initial linear stratification, and that density perturbations are located in a narrow layer which corresponds to a collapsed wake. For  $Nt > Nt_w$  (Fig. 7(c)) we observe density perturbations outside the wake, which are associated with the propagation of random internal waves.

#### 4. Random wave field

In the previous section we have shown that internal waves are predominant inside the wake for  $Nt > Nt_w$ . BCH showed that these waves are also emitted

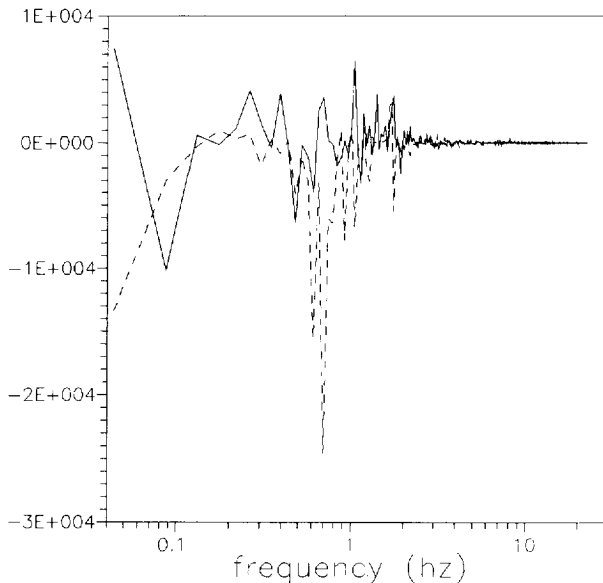


Fig. 9. Co-spectrum (solid line) and quadrature-spectrum (dashed line) between  $\rho'$  measured at  $z = 2R$  and  $z = 5R$ .  $x = 50R$ ,  $F = 6$  ( $Re(1) = 5474$ ,  $R = 5 \text{ cm}$ ).

outside the wake at the same time and demonstrated that these random waves behave like transient internal waves emitted by bodies that are moved impulsively. The phase structure typical of impulsive waves is illustrated in Fig. 8. The shadowgraph side view (Fig. 8(a)) shows, outside the wake, black and white fringes which characterize the random wave isophases. Fig. 8(b) presents a horizontal visualization of these waves which appear as a superposition of semicircular concentric phase line patterns.

To determine the vertical structure of random waves, we have pulled behind the sphere at  $x = 50R$  ( $Nt = 8.3$ ), a set of four conductivity probes located at  $z = 2R$ ,  $3R$ ,  $4R$  and  $5R$ . Spectral analysis of probe signals indicates that whichever  $z$ , wave spectra are dominated by the same frequency which corresponds to the frequency of the wake instability. The phase gap between the signals is due to the slope of the isophases (see Fig. 8(a)). In particular, as shown in Fig. 9, internal waves at  $z = 2R$  and  $5R$  oscillate in phase quadrature. This corresponds to an angle between the vertical and the isophase of  $43^\circ$  which is in agreement with shadowgraph visualizations (Fig. 8(a)).

### Acknowledgements

This work was supported by Météo-France and contract DRET No. 90-233. It was made possible by the Simulation Physique des Ecoulements Atmosphérique (SPEA) team of the French Meteorological Office; thanks to all of them for their kindness and invaluable help.

### References

- Bonneton, P., Chomaz, J.M. and Hopfinger, E., 1993. Internal waves produced by the turbulent wake of a sphere moving horizontally in a stratified fluid. *J. Fluid Mech.*, 245: 23–40.
- Chomaz, J.M., Bonneton, P. and Hopfinger, E., 1993a. The structure of the near wake of a sphere moving horizontally in a stratified fluid. *J. Fluid Mech.*, 245: 1–21.
- Chomaz, J.M., Bonneton, P., Butet, A. and Hopfinger, E., 1993b. Vertical diffusion of the far wake of a sphere moving horizontally in a stratified fluid. *Phys. Fluids*, A5: 2799–2806.
- Lin, Q., Boyer, D.L. and Fernando, H.J.S., 1992a. Turbulent wakes of linearly stratified flow past a sphere. *Phys. Fluids*, A4: 1687–1696.
- Lin, Q., Lindberg, W.R., Boyer, D.L. and Fernando, H.J.S., 1992b. Stratified flow past a sphere. *J. Fluid Mech.*, 240: 315–354.
- Thual, O., Butet, A., Perrier, M. and Hopfinger, E., 1987. Sillage d'une sphère en milieu stratifié. Rapport Direction des Recherches Etudes et Techniques (D.R.E.T.) no. 85/105, Toulouse.